Time-dependent local perturbation in a free-electron gas: Exact results

L. Bönig and K. Schönhammer
Institut für Theoretische Physik, Universität Göttingen, D-3400 Göttingen, Federal Republic of Germany
(Received 28 September 1988)

A localized perturbation moving through a homogeneous electron gas with a constant velocity is studied. The time-dependent Schrödinger equation is solved by means of a Galileo transformation. The energy dissipation rate is expressed in terms of the transport cross section for arbitrary velocities, temperatures, and strength of the perturbation. Expressions for the electron density and the backflow pattern around the moving perturbation are given. Quantitative results are presented for a hard-sphere potential.

I. INTRODUCTION

Electronic excitations play an important role for the frictional losses of particles moving through metal films or scattering from metal surfaces. If the scattering particle has a large mass M, the description of the heavy particle in terms of a classical trajectory often presents a reasonable approximation. To calculate the frictional force due to the creation of electronic excitations in the metal, one has to solve an electronic problem with a localized time-dependent perturbation. Even if the electrons are treated as noninteracting, this generally presents a difficult problem and very few exact results are known.[1] Various authors have treated the model problem of a particle moving with constant velocity through a noninteracting gas.[2,3] When the velocity v of the particle is small compared to the Fermi velocity v_F, the energy dissipation due to the excitation of electron-hole pairs is proportional to v^2 and can be expressed in terms of the phase shifts of the (spherical) potential presented by the heavy particle. Recently one of the authors (K. S.) has shown that these results can easily be generalized to arbitrary velocities v. In the following this publication[4] will be referred to as I. In I the time-dependent Schrödinger equation for the electrons was transformed to a time-independent equation by means of a Galileo transformation. The general expression for the energy dissipation rate in an interacting electron gas is reduced to a simple integral involving one-electron force matrix elements with scattering states for noninteracting electrons. These matrix elements can be expressed in terms of the reflection coefficient $R(p)$ in the one-dimensional case and in terms of the transport cross section $\sigma_{\rm tr}(p)$ or the phase shifts $\delta_l(p)$ in the three-dimensional case. In the latter case numerical work is needed to evaluate the friction coefficient $\eta(v)$, and quantitative results for $\eta(v)$ were presented in I only for the 1D case.

In this paper we present a detailed study of the friction coefficient as a function of velocity and temperature for the case of a hard sphere. As a simple formal expression for the expectation value of an arbitrary one-particle operator can be given, we also present results for the electronic density and the backflow pattern due to the moving perturbation. In Sec. II we give a short but self-contained derivation of the method used in I. Results for the friction coefficient are presented in Sec. III. It is also discussed how the results simplify in the classical limit. Results for the density and the backflow pattern are given in Sec. IV. It is shown that the large-distance behavior of a weak scattering potential cannot be properly described by a linear response theory.[5]

Certainly the model of noninteracting electrons is somewhat academic. But as there exist only very few exact results for time-dependent quantum-mechanical systems with arbitrary strong perturbations, we nevertheless consider it to be useful to present a detailed description of our results. Also recent work on the physics of mesoscopic systems indicates that fully-quantum-mechanical calculations are necessary to describe transport properties in such systems.[6] Some of our results are known in the theory of the stopping power of a *charged* particle in a plasma. The low-velocity result Eq. (17) has, for example, been used for the case of highly degenerate plasma where the transport cross section is evaluated using a screened Coulomb potential.[7]

II. MODEL AND EXACT SOLUTION

We consider a free electron gas with a potential $V_{\mathbf{v}t}=V(\mathbf{x}-\mathbf{v}t)$ localized at $\mathbf{x}=\mathbf{v}t$ and moving with constant velocity $\mathbf{v}$. The Hamiltonian for this model is of the form

$$H_t=H_0+\theta(t-t_0)V_{\mathbf{v}t}\ , \tag{1}$$

where H_0 is the kinetic energy of the electron gas and the potential is switched on at time $t_0<0$. At t_0 the electron gas is assumed to be in an eigenstate of H_0 described by the occupation numbers $n_{\mathbf{p}}$ of the plane-wave states. In the following we denote the Hamiltonian at time $t=0$ by H and the corresponding potential localized in the origin by V, i.e., $H=H_0+V$.

We want to calculate expectation values $\langle\phi(t)|A|\phi(t)\rangle$ where A is an arbitrary one-particle operator and $|\phi(t)\rangle$ is the solution of the time-dependent Schrödinger equation. To solve the Schrödinger equation for $t>t_0$ we perform a Galileo transformation which puts the potential at rest in the origin. The transformed state $|\phi(t)\rangle_T$

$$|\phi(t)\rangle_T \equiv T^{\dagger}_{\mathbf{v},t}|\phi(t)\rangle \tag{2}$$

with the unitary operator

$$T_{\mathbf{v},t} = e^{-i\mathbf{v}\cdot(\hat{\mathbf{P}}t - M_T\hat{\mathbf{X}})/\hbar}, \tag{3}$$

where $\hat{\mathbf{X}}$ is the center-of-mass position operator and M_T is the total mass, obeys the Schrödinger equation

$$i\hbar\frac{d}{dt}|\phi(t)\rangle_T = H|\phi(t)\rangle_T \tag{4}$$

with the *time-independent* Hamiltonian H which has the perturbation located at the origin. Therefore the formal solution of Eq. (4) is trivial. The expectation value of an arbitrary observable A is given by

$$\langle\phi(t)|A|\phi(t)\rangle = \langle\phi(t_0)|T_{\mathbf{v},t_0}e^{iH(t-t_0)/\hbar} \times A_T e^{-iH(t-t_0)/\hbar}T^{\dagger}_{\mathbf{v},t_0}|\phi(t_0)\rangle , \tag{5}$$

where A_T is the transformed observable

$$A_T \equiv T^{\dagger}_{\mathbf{v},t}AT_{\mathbf{v},t} . \tag{6}$$

Using our initial condition Eq. (5) reads for a one-particle operator $A(\hat{\mathbf{x}},\hat{\mathbf{p}})$

$$\langle\phi(t)|A|\phi(t)\rangle = \int n_{\mathbf{p}}\langle\mathbf{p}-m\mathbf{v}|e^{iH(t-t_0)/\hbar} \times A(\hat{\mathbf{x}}+\mathbf{v}t,\hat{\mathbf{p}}+m\mathbf{v})e^{-iH(t-t_0)/\hbar} \times|\mathbf{p}-m\mathbf{v}\rangle d\mathbf{p} , \tag{7}$$

where the momentum states $|\mathbf{p}\rangle$ have the usual δ-function normalization $\langle\mathbf{p}|\mathbf{p}'\rangle=\delta(\mathbf{p}-\mathbf{p}')$. If one is interested in the transient behavior after switching on the potential, complete sets of scattering states $|\mathbf{p}+\rangle$ for the potential V can be inserted and the calculation of the expectation value of A is reduced to integrations. In this paper we only study the stationary behavior at finite times when the limit $t_0\to-\infty$ is performed. The time development operators in Eq. (7) can then be expressed in terms of Møller operators[4] of scattering theory which transform the momentum state $|\mathbf{p}-m\mathbf{v}\rangle$ into scattering states $|(\mathbf{p}-m\mathbf{v})+\rangle$. As the scattering states are eigenstates of H, this leads after averaging over a grand canonical ensemble to

$$\langle\phi(t)|A|\phi(t)\rangle = \int f(\varepsilon_{\mathbf{p}})\langle(\mathbf{p}-m\mathbf{v})+|A(\hat{\mathbf{x}}+\mathbf{v}t,\hat{\mathbf{p}}+m\mathbf{v})|(\mathbf{p}-m\mathbf{v})+\rangle d\mathbf{p} , \tag{8}$$

where $f(\varepsilon_{\mathbf{p}})$ is the Fermi function and $\varepsilon_{\mathbf{p}}=\mathbf{p}^2/2m$. This equation is the basic result of our paper and is studied for various choices of A in the following sections.

III. FRICTION COEFFICIENT

In Sec. III. A we derive general results for the friction coefficient for a three-dimensional spherical potential and present detailed numerical results for a hard sphere in Sec. III B.

A. General results

The rate of energy transfer to the electron gas at time t is given by[4]

$$(\Delta\dot{\varepsilon})_t = \langle\phi(t)|\dot{V}_{\mathbf{v}t}|\phi(t)\rangle . \tag{9}$$

From this energy-transfer rate (ETR) the friction coefficient $\eta(v)$ of a heavy particle of mass M can be calculated,[3]

$$\eta(v) \equiv \frac{(\Delta\dot{\varepsilon})_t}{Mv^2} . \tag{10}$$

Using (8) the ETR can be expressed in terms of force matrix elements[4]

$$(\Delta\dot{\varepsilon})_t = \int f(\varepsilon_{\mathbf{p}}) \times\left\langle(\mathbf{p}-m\mathbf{v})+\left|\left[-\mathbf{v}\cdot\frac{\partial V}{\partial\mathbf{x}}\right]\right|(\mathbf{p}-m\mathbf{v})+\right\rangle d\mathbf{p} . \tag{11}$$

From (11) one can see that the ETR has become time independent.

In the following we discuss the friction coefficient for spherical symmetric potentials V and spinless particles. Then the force matrix elements can be written as

$$\left\langle\mathbf{p}+\left|\mathbf{v}\cdot\frac{\partial V}{\partial\mathbf{x}}\right|\mathbf{p}+\right\rangle = \frac{1}{(2\pi\hbar)^3}\frac{p}{m}(\mathbf{p}\cdot\mathbf{v})\sigma_{\mathrm{tr}}(p) , \tag{12}$$

where $\sigma_{tr}(p)$ is the "transport cross section" defined as

$$\sigma_{\mathrm{tr}}(p) \equiv \int(1-\cos\theta)\sigma_p(\theta)d\Omega \tag{13}$$

and $\sigma_p(\theta)$ is the differential cross section corresponding to V. Details of the derivation of Eq. (12) are given in Appendix A. This leads to

$$(\Delta\dot{\varepsilon})_t = -\int f(\varepsilon_{\mathbf{p}+m\mathbf{v}})(\mathbf{v}\cdot\mathbf{p})\frac{p}{m}\sigma_{\mathrm{tr}}(p)\frac{d\mathbf{p}}{(2\pi\hbar)^3} . \tag{14}$$

As indicated in I for the 1D case this result has a very simple interpretation in terms of the energy transfer in a single binary collision and the corresponding scattering probabilities. This is discussed in Appendix B.

The transport cross section can be expressed in terms of the scattering phase shifts $\delta_l(p)$ using the well-known expression of the differential cross section $\sigma_p(\theta)$ in terms of the phase shifts. This yields

$$\sigma_{\mathrm{tr}}(p) = \frac{4\pi}{(p/\hbar)^2}\sum_{l=0}^{\infty}(l+1)\sin^2[\delta_{l+1}(p)-\delta_l(p)] . \tag{15}$$

The result (14) for the ETR is *exact for arbitrary velocities, temperatures, and strength of the potential.* In various limiting cases this expression can be simplified further. For velocities *small* compared to the Fermi velocity

v_F, the Fermi function can be expanded and leads to an ETR proportional to v^2, i.e.,

$$\eta(v)=\frac{1}{M}\frac{2m^2}{3\pi^2\hbar^3}\int_0^\infty\left[-\frac{\partial f}{\partial\varepsilon}\right]\varepsilon^2\sigma_{\rm tr}(\varepsilon)d\varepsilon\ . \tag{16}$$

At $T=0$ the derivative of the Fermi function is a (negative) δ function and one obtains for $v\ll v_F$

$$\eta(v)=\frac{m}{M}n_0 v_F\sigma_{\rm tr}(p_F)\ , \tag{17}$$

where n_0 is the density of the electron gas and $p_F=mv_F$ is the Fermi momentum. The Fermi velocity v_F is given by

$$v_F=\frac{\hbar}{m}(6\pi^2)^{1/3}n_0^{1/3}\ . \tag{18}$$

For *high* velocities $v\gg\max(v_F,\sqrt{k_BT/m}\,)$ the force matrix element at $\mathbf{p}=m\mathbf{v}$ can be removed from the integrand in (14) and leads to

$$\eta(v)=\frac{m}{M}n_0|v|\sigma_{\rm tr}(m|v|)\ , \tag{19}$$

where we have used $\int f(\varepsilon_{\rm p})d\mathbf{p}=(2\pi\hbar)^3n_0$.

In the *classical limit* $\hbar\to0$ the Fermi function goes over to the Maxwell distribution $\mathcal{W}_0(\varepsilon_{\rm p})$,

$$\frac{f(\varepsilon_{\rm p})}{(2\pi\hbar)^3}\to n_0\mathcal{W}_0(\varepsilon_{\rm p})\ . \tag{20}$$

The transport cross section in (14) has to be replaced by the one evaluated in classical scattering theory. This yields

$$(\Delta\dot{\varepsilon})_t^{\rm cl}=-n_0\int\mathcal{W}_0(\varepsilon_{\rm p+mv})(\mathbf{v}\cdot\mathbf{p})\frac{p}{m}\sigma_{\rm tr}^{\rm cl}(p)d\mathbf{p}\ . \tag{21}$$

At $T=0$ the Maxwell distribution is a δ function and leads to a friction coefficient which vanishes linearly with $|v|$ in contrast to Eq. (17),

$$\eta^{\rm cl}(v)=\frac{m}{M}n_0|v|\sigma_{\rm tr}^{\rm cl}(m|v|)\ . \tag{22}$$

This expression holds generally for $v/\sqrt{k_BT/m}\gg1$. In the opposite limit $v/\sqrt{k_BT/m}\ll1$ the Taylor expansion of the Maxwell distribution in (21) leads to a constant friction coefficient. For the case of a hard sphere (see Sec. III B) the corresponding expression was derived by Cunningham[8] at the beginning of this century and used in his interpolation formula for the theoretical description of Millikan's oil drop experiment.

B. Hard-sphere potential

The transport cross section $\sigma_{\rm tr}(p)$ of a given potential $V(r)$ determines the friction coefficient according to Eqs. (10) and (14). As a function of momentum $\sigma_{\rm tr}(p)$ can have a rich structure. This is shown in Fig. 1 for the case of scattering from a potential hole ("soft attractive sphere"). In the limiting cases discussed in Eqs. (17) and (19) this structure shows up directly in the corresponding friction coefficient. To obtain a simple understanding of Eq. (14) for arbitrary velocities it is desirable to study the result for a "smooth" transport cross section. This is the case for a hard- (inpenetrable) sphere potential. This textbook example[9] allows the exact evaluation of the scattering phase shifts ($k\equiv p/\hbar$)

$$\tan\delta_l(k)=-\frac{j_l(ka)}{n_l(ka)}\ , \tag{23}$$

where a is the radius of the sphere and j_l and n_l are the spherical Bessel functions and Neumann functions. Explicit results for the scattering wave functions are given in Appendix D. The behavior of the total cross section $\sigma_{\rm tot}(p)=\int\sigma_p(\theta)d\Omega$ as a function of p is well known.[9] It starts at $4\pi a^2$, i.e., four times the geometrical cross section, at $p=0$ and decays monotonically to $2\pi a^2$ *(twice* the geometrical cross section) in the limit $p\to\infty$, i.e., the value of the classical cross section $\sigma_{\rm tot}^{\rm cl}(p)=\pi a^2$ is not reached. There is always a cone of small angle in the forward direction within which the scattering is nonclassical. This "anomaly" is suppressed in the transport cross section. Due to the additional factor $(1-\cos\theta)$ the weighting of forward scattering goes to zero and $\sigma_{\rm tr}(p)$ approaches $\sigma_{\rm tr}^{\rm cl}(p)=\pi a^2$ in the limit $p\to\infty$. This is shown in Fig. 2 where $g(x)\equiv\sigma_{\rm tr}(x)/\pi a^2$ is plotted as a function of $x=pa/\hbar$.

We begin our discussion of the friction coefficient with the *zero-temperature* limit. Then $\eta(v)$ has the form

$$\eta(v)=\frac{m}{M}n_0v_F\pi a^2F\left[\frac{v}{v_F},k_Fa\right]\ . \tag{24}$$

Numerical results for the dimensionless function $F=|v|\eta(v)/[v_F\eta^{\rm cl}(v)]$ as a function of v/v_F for various values of k_Fa are shown in Fig. 3. The results smoothly interpolate between the two limiting cases known from Eqs. (17) and (19),

$$F\left[\frac{v}{v_F},k_Fa\right]=\begin{cases}g(k_Fa)\equiv\sigma_{\rm tr}(p_F)/\pi a^2 & \text{for } \dfrac{v}{v_F}\ll1\\[2ex] \dfrac{v}{v_F}g\left[\dfrac{v}{v_F}k_Fa\right] & \text{for } \dfrac{v}{v_F}\gg1\ .\end{cases} \tag{25}$$

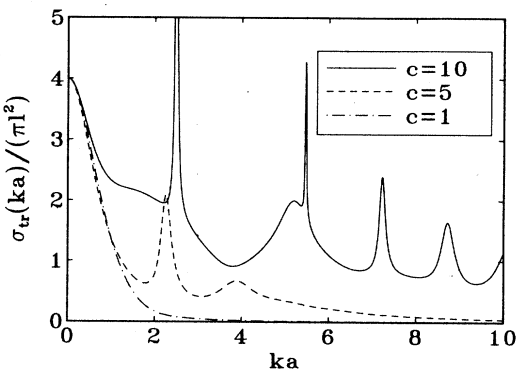

FIG. 1. Normalized transport cross section for a soft attractive sphere as a function of $pa/\hbar=ka$, where a is the sphere radius, $V_0=(\hbar c)^2/2m$ the potential depth, and $l=a[1-\tan(ca)/ca]$ the scattering length.

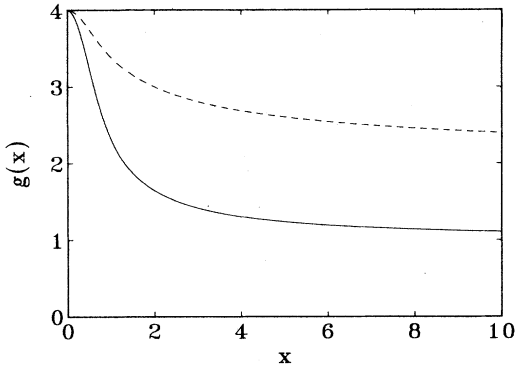

FIG. 2. Normalized transport cross section [solid line: $g(x)\equiv\sigma_{\rm tr}(x)/\pi a^2$, $x\equiv ka$] and total cross section [dashed line: $g(x)\equiv\sigma_{\rm tot}(x)/\pi a^2$] for a hard sphere.

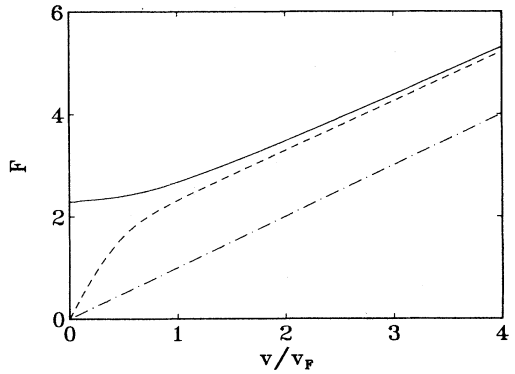

FIG. 4. Comparison of the normalized friction coefficients at zero temperature [Eq. (24)] for the Fermion (solid line), Boson (dashed line), and classical cases (dashed-dotted line).

For sphere radii a small compared to the average distance between electrons ($k_F a \ll 1$) the quantum effects are most pronounced. The different behavior of the quantum-mechanical case [(14)] and the classical case [(21)] is due to two effects: the different momentum distribution and the difference between $\sigma_{\rm tr}$ and $\sigma_{\rm tr}^{\rm cl}$. At $T=0$ a system of noninteracting *bosons* leads to an expression for $\eta(v)$ which is "intermediate" between the classical and the fermion case: the distribution is a δ function as in the classical case, but the quantum-mechanical expression for the transport cross section has to be used. A comparison of all three cases is shown in Fig. 4.

For *finite temperatures* we start with a discussion of the classical friction coefficient. As $\sigma_{\rm tr}^{\rm cl}=\pi a^2$ is independent of p, it can be removed from the integrand in (21). After performing the angular integrations one obtains

$$\eta^{\rm cl}(v)=\frac{m}{M}n_0 v_T \pi a^2 I((v/v_T)^2)\ , \tag{26}$$

where $v_T\equiv\sqrt{2k_BT/m}$ is the thermal velocity and the function $I(\alpha)$ is given by the integral

$$I(\alpha)=\frac{1}{2\sqrt{\pi}}\int_0^\infty x^2[(1+2\alpha x)e^{-\alpha(x+1)^2} -(1-2\alpha x)e^{-\alpha(x-1)^2}]dx\ . \tag{27}$$

In the limit $\alpha\ll 1$ and $\alpha\gg 1$ the function $I(\alpha)$ takes the form

$$I(\alpha)=\begin{cases}\dfrac{8}{3\sqrt{\pi}}\left[1+\dfrac{\alpha}{5}+\mathcal{O}(\alpha^2)\right] & \text{for } \alpha\ll 1\\ \sqrt{\alpha}\left[1+\dfrac{1}{\alpha}+\mathcal{O}\left(\dfrac{1}{\alpha^2}\right)\right] & \text{for } \alpha\gg 1\ .\end{cases} \tag{28}$$

If the value $I(0)$ is used in (26) for small velocities one obtains Cunningham's formula[8] discussed at the end of Sec. III A. The function $I(\alpha)$ is monotonically increasing with α as shown in Fig. 5. Therefore $\eta^{\rm cl}(v)$ increases monotonously as a function of v/v_T, as shown in Fig. 6(a), where for large v/v_T the result (22) is recovered. If $\eta^{\rm cl}\sim\sqrt{T}I(mv^2/2k_BT)$ is plotted as a function of T for fixed v, it increases linearly with T for small T and proportional to $\sqrt{T}$ for large T. This is shown in Fig. 6(b).

In the quantum-mechanical case the condition of fixed

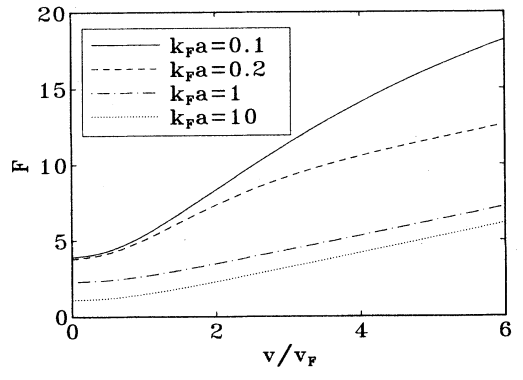

FIG. 3. Normalized friction coefficient F in the zero-temperature limit [Eq. (24)] as a function of v/v_F for various values of $k_F a$.

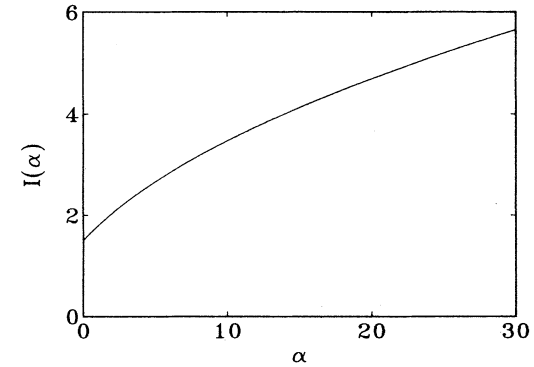

FIG. 5. Dimensionless function $I(\alpha)$ [Eq. (27)] which determines the classical friction coefficient for arbitrary temperatures.

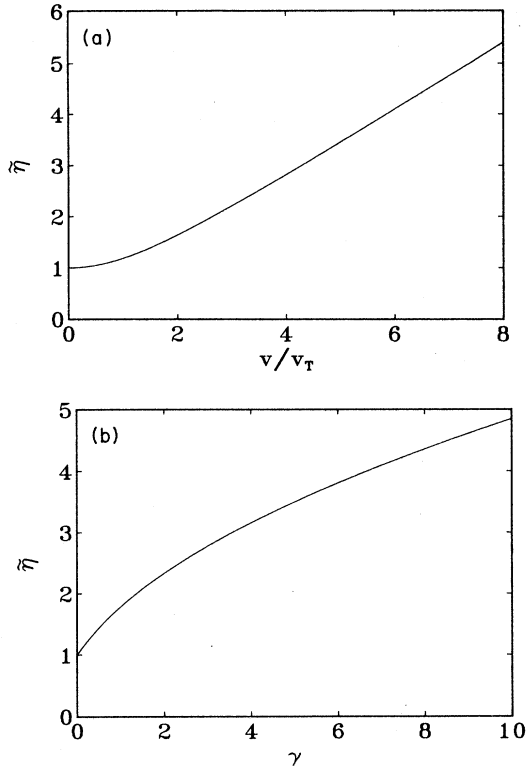

FIG. 6. Reduced classical friction coefficient [Eq. (26)]. 6(a) shows $\tilde{\eta}\equiv(3\sqrt{\pi}/8)I((v/v_T)^2)$ as a function of v/v_T, 6(b) shows $\tilde{\eta}\equiv\sqrt{\gamma}I(1/\gamma)$ as a function of $\gamma\equiv kT/(mv^2/2)$.

particle number determines the chemical potential μ as a function of temperature. With the thermal de Broglie wavelength $\lambda_T\equiv 2\sqrt{\pi}\hbar/mv_T$ it can be expressed in terms of a universal function $G(x)$,

$$\mu(T)=k_B TG(\lambda_T^3 n_0)\ . \tag{29}$$

For $x\ll 1$ one has $G(x)=\ln x$ while for $x\gg 1$ $G(x)$ is proportional to $x^{2/3}$. A plot of $G(x)$ is shown in Fig. 7 where it is compared to the classical value $G(x)=\ln x$ for all values of x.

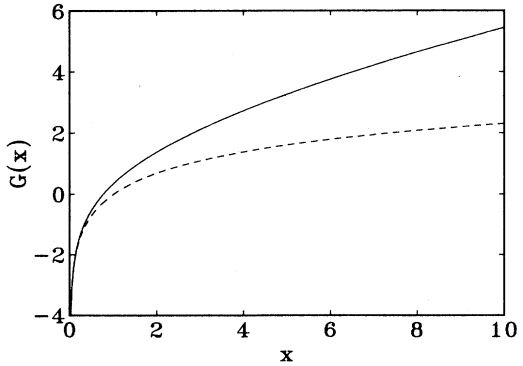

FIG. 7. Universal function $G(x)$ which determines the chemical potential [Eq. (29)] in the Fermion (solid line) and classical cases (dashed line).

In the classical result [Eq. (26)] the radius a of the hard sphere only enters in a factor presenting the geometrical cross section. This is different in the quantum-mechanical case because of the p dependence of the transport cross section $\sigma_{\rm tr}(p)$ shown in Fig. 2. To demonstrate this nontrivial a dependence and the difference between the classical and quantum-mechanical results we show in Fig. 8 the "reduced" friction coefficient $\tilde{\eta}\equiv(M/m)\eta/(n_0\pi a^2)$, which has the dimension of a velocity, as a function of temperature for various values of $v_F\sim n_0^{1/3}$. With units $m=1=\hbar$ we choose the velocity of the hard sphere as the unit velocity $v=1$. For the small value $v_F=0.1$ the Fermi function is "close" to a Maxwell distribution and the curve for $\tilde{\eta}$ looks similar to the classical result in Fig. 6(b). The quantitative difference between Figs. 8(a) and 8(b) is due to the fact that the function $g(x)$ describing the momentum dependence of $\sigma_{\rm tr}$ varies by a factor of 4 between $x=0$ and $x\to\infty$. For $v_F\ll v$ and $v=1$ one obtains from Eq. (19) $\tilde{\eta}(T=0)\approx g(a)$. The ratio of the $\tilde{\eta}$ values for $T=0$ are therefore roughly given by $g(\frac{1}{4})/g(4)\approx 2.9$. For increasing v_F the deviations from the classical result become larger [$\tilde{\eta}(T=0)\approx v_F g(k_F a)$ for $v_F\gg v$] and the temperature dependence of $\tilde{\eta}$ becomes weaker for small temperatures. The classical $\sqrt{T}$ behavior is only reached at very high temperatures. From (16) it is easy to see that the

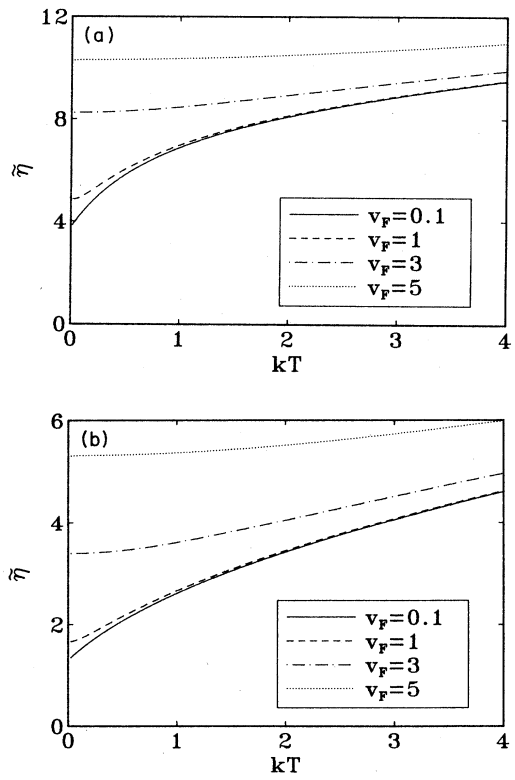

FIG. 8. Reduced friction coefficient $\tilde{\eta}\equiv(M/m)\eta/(n_0\pi a^2)$ in the quantum-mechanical case as a function of the temperature for four different values of the Fermi velocity v_F. We used the units $m=1=\hbar$ and the velocity of the hard sphere $v=1$. For the sphere radius a we choose $a=\frac{1}{4}$ (a) and $a=4$ (b).

quantum-mechanical friction coefficient increases like $(kT)^2$ for small temperatures in the case $v/v_F \ll 1$ which is numerically confirmed (Fig. 8).

IV. DENSITY AND CURRENT DENSITY

In this section we discuss the stationary density and current density in coordinate systems with the perturbation in the origin. This is equivalent of using our general equation (8) at $t=0$. For the expectation value of the density $\hat{\rho}(\mathbf{x})$ this yields with $\psi_{\mathbf{p}}(\mathbf{x}) \equiv \langle \mathbf{x}|\mathbf{p}+\rangle$

$$\langle \hat{\rho}(\mathbf{x}) \rangle = \int f(\varepsilon_{\mathbf{p}+m\mathbf{v}}) |\psi_{\mathbf{p}}(\mathbf{x})|^2 d\mathbf{p} \tag{30}$$

and for the current density $\hat{\mathbf{j}}(\mathbf{x})$

$$\langle \hat{\mathbf{j}}(\mathbf{x}) \rangle = \mathbf{v}\langle \hat{\rho}(\mathbf{x}) \rangle + \frac{\hbar}{m} \mathrm{Im} \left[\int f(\varepsilon_{\mathbf{p}+m\mathbf{v}}) \psi_{\mathbf{p}}^*(\mathbf{x}) \nabla \psi_{\mathbf{p}}(\mathbf{x}) d\mathbf{p} \right] . \tag{31}$$

For $\mathbf{v}=0$ the current density vanishes. Using (A3) for $r \gg a$ the density takes the from $\langle \hat{\rho}(\mathbf{x}) \rangle = n_0 + \delta\rho(\mathbf{x})$ with

$$\delta\rho(\mathbf{x}) = \mathrm{Im} \left[\frac{1}{2\pi^2\hbar^2} \frac{1}{r^2} \int_0^{p_F} e^{2ipr/\hbar} p f_p(-1) dp \right] , \tag{32}$$

where $f_p(-1)$ is the scattering amplitude for backward scattering. This leads to the well-known Friedel oscillations[10]

$$\delta\rho(\mathbf{x}) \sim \cos(2k_F r + \varphi)/r^3 . \tag{33}$$

For the case of the hard sphere the scattering wave functions are explicitly known for all values of r (see Appendix D). For finite values of v the density obtains an angular dependence with different wavelength of the Friedel oscillations in the forward and backward directions. This can be shown analytically for a one-dimensional hard "sphere" (Appendix C) and numerically for a three-dimensional sphere. In the 3D case at $T=0$ it requires a numerical integration over the azimutal angle and the absolute value of the momentum (Appendix D). This leads to the densities shown in Fig. 9.

The numerical effort for $\mathbf{v} \neq 0$ is quite limited for the case of a *Bose gas* at $T=0$. Then the momentum distribution is proportional to $\delta(\mathbf{p})$ and the density is given by $n_0 |\psi_{-m\mathbf{v}}(\mathbf{x})|^2$. A plot of this density is shown in Fig. 10.

Some analytical results can be obtained for the current density *linear in* $\mathbf{v}$. As $\hat{\mathbf{j}}(\mathbf{x})$ is a vector, it has to be a linear combination of the vectors which are available, i.e., $\mathbf{x}$ and $\mathbf{v}$. With the linearity in $\mathbf{v}$ this leads to the form

$$\langle \hat{\mathbf{j}}(\mathbf{x}) \rangle = \mathbf{x}(\mathbf{x}\cdot\mathbf{v}) h_0(r) + \mathbf{v} h_1(r) , \tag{34}$$

where the two functions of $r=|\mathbf{x}|$ have to be calculated from Eq. (31) which simplifies in the linear approximation to

$$\langle \hat{\mathbf{j}}(\mathbf{x}) \rangle = \mathbf{v}\langle \hat{\rho}(\mathbf{x}) \rangle|_{\mathbf{v}=0} + \frac{\hbar}{m} \mathrm{Im} \left[\int (\mathbf{p}\cdot\mathbf{v}) \frac{\partial f}{\partial \epsilon} \psi_{\mathbf{p}}^*(\mathbf{x}) \nabla \psi_{\mathbf{p}}(\mathbf{x}) d\mathbf{p} \right] . \tag{35}$$

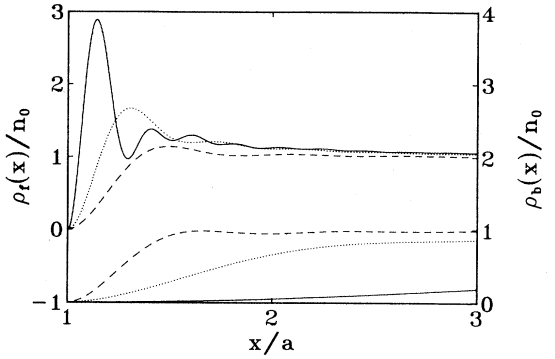

FIG. 9. Density of an electron gas around the hard sphere at zero temperature in the forward (ρ_f) and backward directions (ρ_b) as a function of the distance x. We choose for the Fermi velocity $v_F=5$, the sphere radius $a=1$, and for the velocity of the sphere $v=\frac{1}{2}$ (dashed line), $v=3$ (dotted line), and $v=10$ (solid line). The three upper curves show ρ_f and the three lower show ρ_b.

To calculate the current density near the hard sphere requires a numerical integration (see Appendix D) and the results will be discussed below. For $r \gg a$ we can use the asymptotic form (A3) of the scattering wave functions. Up to terms $\mathcal{O}(1/r^2)$ this yields

$$\frac{\hbar}{i} \psi_{\mathbf{p}}^*(\mathbf{x}) \nabla \psi_{\mathbf{p}}(\mathbf{x}) = \frac{1}{(2\pi\hbar)^3} \left[\mathbf{p} + p\hat{\mathbf{x}} f_p \frac{e^{ipr/\hbar} e^{-i\mathbf{p}\cdot\mathbf{x}/\hbar}}{r} + \mathbf{p} f_p^* \frac{e^{-ipr/\hbar} e^{i\mathbf{p}\cdot\mathbf{x}/\hbar}}{r} + p\hat{\mathbf{x}} \frac{|f_p|^2}{r^2} \right] . \tag{36}$$

We should note that (36), as it stands, is not systematic up to terms of order $1/r^2$, as we have neglected in (A3) the term of $\psi_{\mathbf{p}}$ which is proportional to $1/r^2$. It is easy to show that the corresponding term does not contribute to

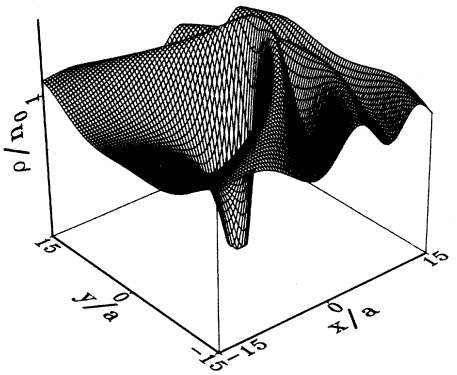

FIG. 10. Density of a Bose gas at $T=0$. In the picture the sphere moves to the right in the x direction with velocity $v=\frac{1}{2}$. The normalized density is plotted in the z direction.

leading order in $1/r$ after the $\mathbf{p}$ integration in (35) is performed. This leading-order behavior is obtained by partial integrations in the angular integral in (35) for the second and the third term on the rhs of (36). This yields

$$\langle \hat{\mathbf{j}}(\mathbf{x}) \rangle = \frac{\hat{\mathbf{x}}(\hat{\mathbf{x}}\cdot\mathbf{v})}{r^2} \int_0^\infty \left[-\frac{\partial f}{\partial \varepsilon} \right] \frac{p^4}{m} \sigma_{\mathrm{tr}}(p) \frac{dp}{(2\pi\hbar)^3} + \mathcal{O}\left[\frac{1}{r^3}\right] . \tag{37}$$

The leading order contribution is *purely radial,* i.e., the function $h_1(r)$ in Eq. (34) vanishes like r^{-3} for large distances. For *weak* potentials V the transport cross section is proportional to V^2. Therefore it is obvious that the $1/r^2$ contribution to the current density *cannot be obtained by linear response theory.* In linear response one gets a dipolar backflow pattern at large distances as discussed by Pines and Nozières.[5] They obtain

$$\langle \hat{\mathbf{j}}(\mathbf{x}) \rangle_{\mathrm{LR}} \sim V_0 \nabla(\mathbf{v}\cdot\nabla)\frac{1}{r} , \tag{38}$$

where V_0 is the $\mathbf{q}=0$ Fourier component of the potential. This "hydrodynamic"-like backflow pattern does *not* provide the correct behavior of the current density at large distances for the free-electron gas. For every finite value of the potential the behavior (37) dominates at large enough distances from the perturbation. We mention that the $1/r^2$ term in the large-r expansion of $\psi_{\mathbf{p}}(x)$ in (A3) is needed to obtain the linear response result (38) starting from Eq. (31). The asymptotic result (37) is also confirmed by our numerical evaluation of Eq. (35) for arbitrary values of r. Some additional details of the calculation are given in Appendix D. In Fig. 11 we show the radial component j_r of the current density in the $\mathbf{v}$ direction as well as the angular component j_θ in the direction perpendicular to $\mathbf{v}$. These two plots completely determine the functions h_0 and h_1 in Eq. (34). A "qualitative" picture of the backflow pattern near the sphere is shown in Fig. 12. We have not performed calculations of $\langle \hat{\mathbf{j}}(\mathbf{x}) \rangle$ for arbitrary values of $\mathbf{v}$ as they are numerically more time consuming.

For noninteracting *bosons* at $T=0$ the calculation of

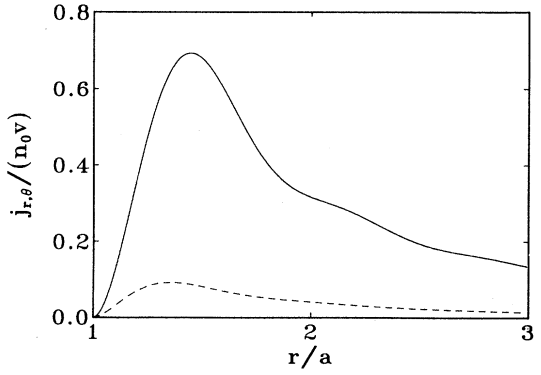

FIG. 11. Radial component j_r (solid line) of the current density in the $\mathbf{v}$ direction and negative azimutal component j_Θ (dashed line) in the direction perpendicular to $\mathbf{v}$. We used the parameters $v_F=5$ and $a=1$.

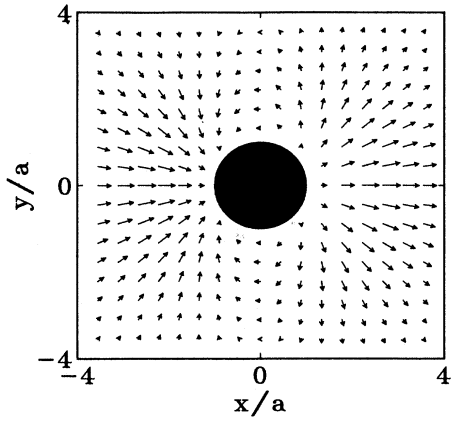

FIG. 12. Current density of an electron gas around the hard sphere at zero temperature in the linear approximation [Eq. (D4)]. The sphere moves to the right in the x direction. For the parameters we choose $a=1$ and $v_F=1$. The length of the arrows gives the absolute value of the current density times an arbitrary scaling factor.

the current density for arbitrary velocities is easy. For $r \gg a$ one obtains

$$\langle \hat{\mathbf{j}}(\mathbf{x}) \rangle_B = \frac{1}{(2\pi\hbar)^3}\frac{1}{r}(v\hat{\mathbf{x}}+\mathbf{v}) \times \mathrm{Re}[f_{mv}(\hat{\mathbf{x}}\cdot\hat{\mathbf{p}})e^{im(vr+\mathbf{v}\cdot\mathbf{x})/\hbar}] + \mathcal{O}\left[\frac{1}{r^2}\right] . \tag{39}$$

V. CONCLUDING REMARKS

We have presented exact results for various expectation values of observables of a free-electron gas in the presence of a localized time-dependent perturbation of arbitrary strength and moving with arbitrary velocities. To make contact to realistic systems it would be necessary to include the electron-electron interaction in the calculation. Some of the results presented in I hold also in this more general case. To further evaluate these formal results it seems necessary to use standard many-body techniques. Another interesting area of further research is to go from the case of the infinitely heavy perturbation treated in this paper to a description which includes the dynamics ("recoil") of a very heavy particle of mass M. In the path-integral description of such a system the coupling to the "electron bath" is usually described in perturbation theory or in the adiabatic approximation,[11] i.e., not as general as in the $M=\infty$ limit discussed in our paper.

APPENDIX A

In this appendix we present two different derivations of the relation [Eq. (12)] between the force matrix elements and the transport cross section $\sigma_{\mathrm{tr}}(p)$. First we start from the time-independent Schrödinger equation for the scattering wave function $\psi_{\mathbf{p}}(\mathbf{x}) \equiv \langle \mathbf{x}|\mathbf{p}+\rangle$ and differentiate it with respect to x_i. This leads to

$$\psi_p^* \frac{\partial V}{\partial x_i}\psi_p = \frac{\hbar^2}{2m}\left[\psi_p^* \nabla^2 \frac{\partial \psi_p}{\partial x_i} - \frac{\partial \psi_p}{\partial x_i}\nabla^2 \psi_p^*\right] . \tag{A1}$$

By Green's theorem the force matrix element can then be expressed as a surface integral over a large sphere

$$\left\langle \mathbf{p}+ \left| \frac{\partial V}{\partial x_i} \right| \mathbf{p}+ \right\rangle = \int \frac{\hbar^2}{2m}\left[\psi_p^* \frac{\partial}{\partial r}\left[\frac{\partial \psi_p}{\partial x_i}\right] - \frac{\partial \psi_p}{\partial x_i}\frac{\partial \psi_p^*}{\partial r}\right] dS . \tag{A2}$$

For large $\mathbf{x}$ the scattering wave function can be expressed in terms of the scattering amplitude $f_p(\hat{\mathbf{x}}\cdot\hat{\mathbf{p}})$, where $\hat{\mathbf{x}}$ and $\hat{\mathbf{p}}$ are unit vectors in the directions $\mathbf{x}$ and $\mathbf{p}$,

$$\psi_p(\mathbf{x}) = \frac{1}{(2\pi\hbar)^{3/2}}\left[e^{i\mathbf{p}\cdot\mathbf{x}/\hbar} + f_p(\hat{\mathbf{x}}\cdot\hat{\mathbf{p}})\frac{e^{ipr/\hbar}}{r} + \mathcal{O}\left[\frac{1}{r^2}\right]\right] . \tag{A3}$$

Straightforward differentiation leads to

$$\begin{aligned}\left\langle \mathbf{p}+ \left| \mathbf{v}\cdot\frac{\partial V}{\partial \mathbf{x}} \right| \mathbf{p}+ \right\rangle = -\frac{p/m}{(2\pi\hbar)^3}\lim_{r\to\infty}\int [&(\mathbf{p}\cdot\mathbf{v})(\hat{\mathbf{p}}\cdot\hat{\mathbf{x}})r^2 + p\,\mathbf{v}\cdot\hat{\mathbf{x}}|f_p(\hat{\mathbf{x}}\cdot\hat{\mathbf{p}})|^2 \\ &+\tfrac{1}{2}\mathbf{p}\cdot\mathbf{v}r(1+\hat{\mathbf{p}}\cdot\hat{\mathbf{x}})f_p^*(\hat{\mathbf{x}}\cdot\hat{\mathbf{p}})e^{-ipr/\hbar}e^{i\mathbf{p}\cdot\mathbf{x}/\hbar} \\ &+\tfrac{1}{2}\mathbf{x}\cdot\mathbf{v}p(1+\hat{\mathbf{p}}\cdot\hat{\mathbf{x}})f_p(\hat{\mathbf{x}}\cdot\hat{\mathbf{p}})e^{ipr/\hbar}e^{-i\mathbf{p}\cdot\mathbf{x}/\hbar}]d\Omega_{\mathbf{x}} .\end{aligned} \tag{A4}$$

The integrand on the rhs of (A4) can be simplified using

$$\int (\mathbf{v}\cdot\hat{\mathbf{x}})f(\hat{\mathbf{x}}\cdot\hat{\mathbf{p}},r)d\Omega_{\mathbf{x}} = (\mathbf{v}\cdot\hat{\mathbf{p}})\int(\hat{\mathbf{p}}\cdot\hat{\mathbf{x}})f(\hat{\mathbf{x}}\cdot\hat{\mathbf{p}},r)d\Omega_{\mathbf{x}} , \tag{A5}$$

which holds for arbitrary functions $f(\hat{\mathbf{x}}\cdot\hat{\mathbf{p}},r)$. The first term on the rhs of (A4) integrates to zero and one obtains

$$\left\langle \mathbf{p}+ \left| \mathbf{v}\cdot\frac{\partial V}{\partial \mathbf{x}} \right| \mathbf{p}+ \right\rangle = -\frac{p}{m}\frac{\mathbf{p}\cdot\mathbf{v}}{(2\pi\hbar)^3}\lim_{r\to\infty}\int\left[\hat{\mathbf{p}}\cdot\hat{\mathbf{x}}|f_p(\hat{\mathbf{x}}\cdot\hat{\mathbf{p}})|^2 + \frac{r}{2}(1+\hat{\mathbf{p}}\cdot\hat{\mathbf{x}})[f_p^*(\hat{\mathbf{x}}\cdot\hat{\mathbf{p}})e^{-ipr/\hbar}e^{i\mathbf{p}\cdot\mathbf{x}/\hbar} + \text{c.c.}]\right]d\Omega_{\mathbf{x}} . \tag{A6}$$

If a partial integration is performed in the angular integration of the second term of the integrand, the corresponding contribution to the integral can be expressed in terms of the imaginary part of the forward scattering amplitude in the limit $r\to\infty$. Using the optical theorem this finally leads to Eq. (12).

A more direct approach to derive Eq. (12) is obtained by use of the Lippmann-Schwinger equation[9] (LSE)

$$|\mathbf{p}+\rangle = |\mathbf{p}\rangle + G_0(\varepsilon_p + i0)V|\mathbf{p}+\rangle , \tag{A7}$$

where $G_0(z)=(z-H_0)^{-1}$ is the unperturbed resolvent. The force matrix element can be expressed as a commutator of V with the momentum operator $\hat{\mathbf{p}}$,

$$\left\langle \mathbf{p}+ \left| \mathbf{v}\cdot\frac{\partial V}{\partial \mathbf{x}} \right| \mathbf{p}+ \right\rangle = \frac{i}{\hbar}\langle \mathbf{p}+|[\hat{\mathbf{p}}\cdot\mathbf{v}, V]|\mathbf{p}+\rangle . \tag{A8}$$

Now we use the LSE for $\langle \mathbf{p}+|$ in the first term of the commutator and for $|\mathbf{p}+\rangle$ in the second term. This leads with $[G_0,\hat{\mathbf{p}}]=0$ to

$$\begin{aligned}\left\langle \mathbf{p}+ \left| \mathbf{v}\cdot\frac{\partial V}{\partial \mathbf{x}} \right| \mathbf{p}+ \right\rangle &= \frac{i}{\hbar}[(\mathbf{p}\cdot\mathbf{v})(\langle \mathbf{p}|V|\mathbf{p}+\rangle - \langle \mathbf{p}+|V|\mathbf{p}\rangle) \\ &\quad + 2\pi i\langle \mathbf{p}+|V(\mathbf{v}\cdot\hat{\mathbf{p}})\delta(\varepsilon_p - H_0)V|\mathbf{p}+\rangle] .\end{aligned} \tag{A9}$$

The first term on the rhs is proportional to the imaginary part of the scattering amplitude. Using the LSE again this term can be brought into a form similar to the second term. Inserting a complete set of plane-wave states $|\mathbf{p}'\rangle$ between the V operators leads to

$$\left\langle \mathbf{p}+ \left| \mathbf{v}\cdot\frac{\partial V}{\partial \mathbf{x}} \right| \mathbf{p}+ \right\rangle = \frac{2\pi}{\hbar}\int |\langle \mathbf{p}'|V|\mathbf{p}+\rangle|^2 \mathbf{v}\cdot(\mathbf{p}-\mathbf{p}')\delta(\varepsilon_p - \varepsilon_{p'})d\mathbf{p}' . \tag{A10}$$

If we denote the differential cross section for scattering

from $\mathbf{p}=p\mathbf{n}$ to $\mathbf{p}'=p\mathbf{n}'$ by $\sigma_p(\mathbf{n}',\mathbf{n})$ we obtain for general potentials V

$$\left\langle \mathbf{p}+\left|\mathbf{v}\cdot\frac{\partial V}{\partial \mathbf{x}}\right|\mathbf{p}+\right\rangle = \frac{p}{m}\frac{1}{(2\pi\hbar)^3}\int \mathbf{v}\cdot(\mathbf{p}-\mathbf{p}')\sigma_p(\mathbf{n}',\mathbf{n})d\mathbf{n}' \ . \quad \text{(A11)}$$

For spherical potentials σ_p depends on $\mathbf{n}'$ and $\mathbf{n}$ only via $\mathbf{n}'\cdot\mathbf{n}$. Then (A11) leads with (A5) to Eq. (12).

APPENDIX B

In this appendix we show that the stationary ($t_0\to-\infty$) result for the ETR for a spherical potential presented in Eq. (14) can be given a very simple interpretation in terms of the energy transfer in a single binary collision and the corresponding scattering probabilities. The derivation of Eq. (14) presented in I and this paper can therefore be considered as a *proof* of the widely held belief that such a use of *probabilities* instead of probability amplitudes is allowed under special circumstances. Limitations of this approach are pointed out for more general potentials.

The momentum $\mathbf{p}$ of an electron can be decomposed as $\mathbf{p}=m\mathbf{v}+\tilde{\mathbf{p}}$, where $\tilde{\mathbf{p}}$ is the momentum in the "center-of-mass" system moving with the perturbation. If an "electron" is scattered from $\mathbf{p}$ to $\mathbf{p}'$, this leads to an energy transfer

$$\Delta E=\frac{1}{2m}(\mathbf{p}'^2-\mathbf{p}^2)=\mathbf{v}\cdot(\tilde{\mathbf{p}}'-\tilde{\mathbf{p}}) \quad \text{(B1)}$$

as the scattering is elastic ($|\tilde{\mathbf{p}}'|=|\tilde{\mathbf{p}}|$). The total energy-transfer rate using scattering probabilities is given by

$$(\Delta\dot{E})_t=\int \mathbf{v}\cdot(\tilde{\mathbf{p}}'-\tilde{\mathbf{p}})N(\tilde{p}\tilde{\mathbf{n}}'\leftarrow\tilde{\mathbf{p}})d\tilde{\mathbf{p}}\,d\tilde{\mathbf{n}}' \ , \quad \text{(B2)}$$

where $N(\tilde{p}\tilde{\mathbf{n}}'\leftarrow\tilde{\mathbf{p}})$ is the rate of scattering events from $\tilde{\mathbf{p}}$ to $\tilde{\mathbf{p}}'=\tilde{p}\tilde{\mathbf{n}}'$ and $\tilde{\mathbf{n}}'$ is the unit vector in the scattered direction. This rate can be expressed in terms of the differential cross section $\sigma_p(\tilde{\mathbf{n}}'\cdot\tilde{\mathbf{n}})$,

$$N(\tilde{\mathbf{p}}'\leftarrow\tilde{\mathbf{p}})=n_0\frac{\tilde{p}}{m}\sigma_{\tilde{p}}(\tilde{\mathbf{n}}'\cdot\tilde{\mathbf{n}})P(\tilde{\mathbf{p}})[1+\alpha P(\tilde{\mathbf{p}}')] \ , \quad \text{(B3)}$$

where $P(\tilde{\mathbf{p}})$ is the normalized probability density for the initial state to be occupied. The factor $\tilde{p}/m$ takes care of the fact that collisions with high relative velocity are more frequent. The constant α is the last factor on the rhs of (B3) depends on the statistics of the particles. Actually the value of α turns out to be irrelevant for the case discussed, as the term proportional to α does not contribute to the ETR given by (B2) because the corresponding integrand is antisymmetric in $\tilde{\mathbf{n}}$ and $\tilde{\mathbf{n}}'$. For noninteracting fermions the probability distribution $P(\tilde{\mathbf{p}})$ is proportional to the shifted Fermi function

$$P(\tilde{\mathbf{p}})=\frac{f(\varepsilon_{\tilde{\mathbf{p}}+m\mathbf{v}})}{n_0(2\pi\hbar)^3} \ . \quad \text{(B4)}$$

This leads to

$$(\Delta\dot{E})_t=\int \mathbf{v}\cdot(\tilde{\mathbf{p}}'-\tilde{\mathbf{p}})\frac{\tilde{p}}{m}\sigma_{\tilde{p}}(\tilde{\mathbf{n}}\cdot\tilde{\mathbf{n}}')f(\varepsilon_{\tilde{\mathbf{p}}+m\mathbf{v}})\frac{d\tilde{\mathbf{p}}}{(2\pi\hbar)^3}d\tilde{\mathbf{n}}' \ . \quad \text{(B5)}$$

The $\tilde{\mathbf{n}}'$ integration can be carried out and leads with (A5) and (13) to the result for the ETR presented in Eq. (14).

If the scattering potential is *not* spherical the differential cross section $\sigma_p(\tilde{\mathbf{n}}'\cdot\tilde{\mathbf{n}})$ depends on $\tilde{\mathbf{n}}$ and $\tilde{\mathbf{n}}'$ separately. Then Eq. (B5) with $\sigma_p(\tilde{\mathbf{n}}'\cdot\tilde{\mathbf{n}})$ replaced by $\sigma_p(\tilde{\mathbf{n}}',\tilde{\mathbf{n}})$ follows from (B2) and (B3) only if σ_p is symmetric in $\tilde{\mathbf{n}}'$ and $\tilde{\mathbf{n}}$. In the absence of a magnetic field this is guaranteed if the potential V has inversion symmetry $V(\mathbf{x})=V(-\mathbf{x})$. This condition shows the restricted validity of the "probabilistic approach" in the quantum-mechanical case, i.e., for nonvanishing α. The *exact* solution for the ETR given by Eqs. (11) and (A11) is *linear* in the electron distribution, while the probabilistic approach of this appendix leads to an additional bilinear term in the distribution if the potential has no inversion symmetry.

APPENDIX C

In this appendix we discuss the electron density in the 1D case for *arbitrary velocities* v and zero temperature at time $t=0$, i.e., when the potential $V(x)$ is located in the origin. We assume the potential to be nonzero only for $|x|\le a$. According to Eq. (8) the density at $T=0$ is determined by the scattering wave functions $\psi_p(x)\equiv\langle x|p+\rangle$,

$$\langle\hat{\rho}(x)\rangle=\int_{-p_F-mv}^{p_F-mv}|\psi_p(x)|^2dp \ , \quad \text{(C1)}$$

where $p_F>0$ is the Fermi momentum. In the following we assume that $v>0$. For $p>0$ the scattering wave functions have the form

$$\psi_p(x)=\frac{1}{(2\pi\hbar)^{1/2}}\begin{cases}e^{ipx/\hbar}+A_p e^{-ipx/\hbar}, & x<-a\\ B_p e^{ipx/\hbar}, & x>a\end{cases} \quad \text{(C2)}$$

while for negative momentum one obtains

$$\psi_{-|p|}(x)=\frac{1}{(2\pi\hbar)^{1/2}}\begin{cases}\tilde{B}_p e^{-ipx/\hbar}, & x<-a\\ e^{-ipx/\hbar}+\tilde{A}_p e^{ipx/\hbar}, & x>a\end{cases} \quad \text{(C3)}$$

where $\tilde{A}_p=-A_p^*(B_p/B_p^*)$ and $\tilde{B}_p=B_p$ by time reversal invariance. We introduce the phases α_p and $\tilde{\alpha}_p$ by

$$A_p\equiv|A_p|e^{i\alpha_p}, \quad \tilde{A}_p\equiv|A_p|e^{i\tilde{\alpha}_p} \ . \quad \text{(C4)}$$

To calculate the density $\langle\hat{\rho}(x)\rangle$ we have to distinguish the cases $v<v_F$ and $v\ge v_F$. With the reflection coefficient $R(p)\equiv|A_p|^2$ Eqs. (C1)–(C3) lead for $v<v_F$ to

$$\langle\hat{\rho}(x)\rangle-n_0=\frac{1}{2\pi\hbar}\begin{cases}-\int_{p_F-mv}^{p_F+mv}R(p)dp+2\int_0^{p_F-mv}\sqrt{R(p)}\cos(2px/\hbar-\alpha_p)dp, & x<-a\\ \int_{-p_F-mv}^{-p_F+mv}R(p)dp+2\int_{-p_F-mv}^{0}\sqrt{R(p)}\cos(2px/\hbar+\tilde{\alpha}_p)dp, & x>a\end{cases} \tag{C5}$$

and for $v\geq v_F$

$$\langle\hat{\rho}(x)\rangle-n_0=\frac{1}{2\pi\hbar}\begin{cases}-\int_{-p_F-mv}^{p_F-mv}R(p)dp, & x<-a\\ \int_{-p_F-mv}^{p_F-mv}R(p)dp+2\int_{-p_F-mv}^{p_F-mv}\sqrt{R(p)}\cos(2px/\hbar+\tilde{\alpha}_p)dp, & x>a\ .\end{cases} \tag{C6}$$

Explicit expressions can be given for an infinitely high square-well potential which has a unit reflection coefficient $R(p)=1$ and $\alpha_p=\pi-2pa/\hbar=\tilde{\alpha}_p$. Then the integrations in (C5) and (C6) can be easily performed and yield for $v<v_F$

$$\langle\hat{\rho}(x)\rangle=\begin{cases}n_0\left[1-\frac{v}{v_F}\right]-\frac{1}{2\pi(x+a)}\sin\left[\frac{2(p_F-mv)(x+a)}{\hbar}\right], & x<-a\\ n_0\left[1+\frac{v}{v_F}\right]-\frac{1}{2\pi(x-a)}\sin\left[\frac{2(p_F+mv)(x-a)}{\hbar}\right], & x>a\end{cases} \tag{C7}$$

and for $v\geq v_F$

$$\langle\hat{\rho}(x)\rangle=\begin{cases}0, & x<-a\\ 2n_0-\frac{1}{\pi}\frac{1}{x-a}\cos\left[\frac{2mv(x-a)}{\hbar}\right]\sin[2k_F(x-a)], & x>a\ .\end{cases} \tag{C8}$$

These results have a simple interpretation. All electrons are totally reflected from the infinitely high barrier. For $v<v_F$ a fraction $(1-v/v_F)$ of the "right-moving" electrons is faster than the perturbation and the density to the left of the perturbation is diminished accordingly while to the right it is increased by the total reflection. The Friedel oscillations presented by the second term on the rhs of (C7) have different wavelengths ("Doppler shift") in front and behind the perturbation. For $v>v_F$ the density behind the potential is zero as it started to move in the infinite past.

APPENDIX D

The purpose of this appendix is to derive explicit expressions for the density and current density, which were used in the numerical calculations. We consider a free-electron gas at zero temperature. The scattering wave functions can be expressed in terms of radial wave functions $f_{l,p}(r)$

$$\psi_{\mathbf{p}}(\mathbf{x})=\frac{1}{(2\pi\hbar)^{3/2}}\sum_{l=0}^{\infty}(2l+1)i^l f_{l,p}(r)P_l(\hat{\mathbf{x}}\cdot\hat{\mathbf{p}})\ , \tag{D1}$$

where P_l is the Legendre polynomial of degree l. For a hard-sphere potential the exact radial functions are

$$f_{l,p}(r)=\frac{j_l(pr)n_l(pa)-j_l(pa)n_l(pr)}{n_l(pa)+ij_l(pa)}\ . \tag{D2}$$

As we mentioned in Sec. IV, the numerical calculation of the density at $T=0$ in front and behind a three-dimensional hard sphere requires a double integration

$$\langle\hat{\rho}(\mathbf{x})\rangle=\frac{1}{4\pi^2\hbar^3}\int_{\max(0,mv-p_F)}^{mv+p_F}dp\,p^2\int_{-1}^{[p_F^2-p^2-(mv)^2]/(2mvp)}du\left|\sum_{l=0}^{\infty}(2l+1)i^l f_{l,p}(r)P_l(\pm u)\right|^2, \tag{D3}$$

where we used (30) and (D1). The upper (lower) sign corresponds to the forward (backward) direction.

From (35) the current density for $T=0$ can be obtained,

$$\langle\hat{\mathbf{j}}(\mathbf{x})\rangle=\mathbf{v}\langle\hat{\rho}(\mathbf{x})\rangle|_{v=0}-\hbar p_F^2\,\mathrm{Im}\left[\int(\hat{\mathbf{p}}\cdot\mathbf{v})\psi_{\mathbf{p}}^*(\mathbf{x})\nabla\psi_{\mathbf{p}}(\mathbf{x})d\Omega_{\mathbf{p}}\right]. \tag{D4}$$

It is useful to split the current density into its radial and azimutal component. Together with (A5) and (D1) this yields for j_r

$$\langle j_r(\mathbf{x})\rangle=(\hat{\mathbf{x}}\cdot\mathbf{v})\left[\langle\hat{\rho}(\mathbf{x})\rangle|_{\mathbf{v}=0}+\frac{p_F^2}{2\pi^2\hbar^2}\mathrm{Re}\sum_{l=0}^{\infty}(l+1)[f^*_{l+1,p_F}(r)f'_{l,p_F}(r)-f^*_{l,p_F}(r)f'_{l+1,p_F}(r)]\right] \tag{D5}$$

and for j_θ

$$\langle j_\theta(\mathbf{x})\rangle=(\mathbf{e}_\theta\cdot\mathbf{v})\left[\langle\hat{\rho}(\mathbf{x})\rangle|_{\mathbf{v}=0}-\frac{\hbar p_F^2\pi}{r}\mathrm{Im}\left[\int_0^{\pi}\sin^3\theta_p\psi^*_{\mathbf{p}}(\mathbf{x})\frac{\partial}{\partial(\cos\theta_p)}\psi_{\mathbf{p}}(\mathbf{x})d\theta_p\right]\right]. \tag{D6}$$

The derivative of the scattering wave function in (D6) is given by

$$\frac{\partial}{\partial(\cos\theta_p)}\psi_{\mathbf{p}}(\mathbf{x})=\frac{1}{(2\pi\hbar)^{3/2}}\frac{1}{\sin^2\theta_p}\sum_{l=0}^{\infty}(2l+1)li^l f_{l,p}(r)[P_{l-1}(\cos\theta_p)-\cos\theta_p P_l(\cos\theta_p)]\,. \tag{D7}$$

[1]For a review, see K. Schönhammer and O. Gunnarsson, in *Many Body Phenomena at Surfaces,* edited by D. Langreth and H. Suhl (Academic, Orlando 1984); A. Yoshimory and K. Makoshi, Prog. Surf. Sci. **21**, 209 (1986).

[2]A. Blandin, A. Nourtier, and D. W. Hone, J. Phys. (Paris) **37**, 369 (1976).

[3]E. G. d'Agliano, P. Kumar, W. Schaich, and H. Suhl, Phys. Rev. B **11**, 2122 (1975).

[4]K. Schönhammer, Phys. Rev. B **37**, 7735 (1988).

[5]D. Pines and P. Nozières, *The Theory of Quantum Liquids* (Benjamin, New York, 1966), pp. 128–130.

[6]For a review, see, e.g., Y. Imry, in *Directions in Condensed Matter Physics,* edited by G. Grinstein and G. Mazenko (World Scientific, Singapore, 1986), pp. 101–163.

[7]T. H. Ferrel and R. H. Ritchie, Phys. Rev. B **16**, 115 (1977); L. Ferrariis and N. Arista, Phys. Rev. A **29**, 2145 (1984).

[8]E. Cunningham, Proc. R. Soc. **83**, 357 (1910); unfortunately there are misprints in his final formula.

[9]N. Mott and H. Massey, *The Theory of Atomic Collisions* (Clarendon, Oxford, 1965), pp. 38–40.

[10]C. Kittel, *Quantum Theory of Solids* (Wiley, New York, 1963), p. 348.

[11]Y. C. Chen, J. Stat. Phys. **49**, 811 (1987).